Novel dynamical behaviors of interaction solutions of the (3+1)-dimensional generalized B-type Kadomtsev-Petviashvili model

Article *in* Physica Scripta · December 2021

DOI: 10.1088/1402-4896/abecf9

M. Belal Hossen
Uttara University

Harun-Or-Roshid Roshid
Sunamgonj Science and Technology University Shantiganj

IOP Publishing Phys. Scr. 96 (2021) 125236 https://doi.org/10.1088/1402-4896/abecf9

Physica Scripta

PAPER

RECEIVED
16 February 2021

ACCEPTED FOR PUBLICATION
9 March 2021

PUBLISHED
22 October 2021

Novel dynamical behaviors of interaction solutions of the (3 + 1)-dimensional generalized B-type Kadomtsev-Petviashvili model

M Belal Hossen[1,2,*], Harun-Or Roshid[3], M Zulfikar Ali[2] and Hadi Rezazadeh[4]

[1] Department of Computer Science & Engineering, Uttara University, Bangladesh
[2] Department of Mathematics, Rajshahi University, Bangladesh
[3] Department of Mathematics, Pabna University of Science and Technology, Bangladesh
[4] Faculty of Engineering Technology, Amol University of Special Modern Technologies, Amol, Iran
[*] Author to whom any correspondence should be addressed.

E-mail: belalshimul14@gmail.com, harunorroshidmd@gmail.com, zulfi1022002@yahoo.com and rezazadehadi1363@gmail.com

Keywords: The generalized B-type Kadomtsev-Petviashvili model, Hirota's bilinear form, interaction, lump waves, kink waves, periodic waves

Abstract

This article is devoted to determine interactions of lump and various solitary wave solutions of the generalized (3 + 1)-D B-type Kadomtsev-Petviashvili (BKP) model which is frequently arises in fluid dynamics, plasma physics, and feebly dispersive media. Bearing in mind on the bilinear formalism and symbolic software Maple-18, we determine three types of interaction solutions of the model. The first type of interaction occurs between a lump wave and a stripe soliton exhibits elastic collisions. Second type of collision between exponential and trigonometric functions generates periodic lump type breather wave solutions. Besides this, the breather wave degenerate into a single lump wave is determined by using parametric limit scheme. Thirdly, we reflect a new interaction solution among lump, kink and periodic waves via 'rational-cosh-cos' type test function. Four different conditions on the exits parameters are illustrated with fission properties in the third case. In addition, we display the dynamical characteristics of the interaction solutions to reveal the evolutions and flow directions via 3D and contour profiles of the model.

1. Introduction

Recently, finding accurate collision solutions of nonlinear partial differential equations (NLPDEs) are an essential issue in soliton theory. In recent years, scientists have been investing their research effort to study of soliton solution of NLEEs. A number of powerful methods were presented such as the inverse scattering transform [1], the Darboux transformation [2], the Backlund transformation [3], the modified double sub-equation method [4], the unified method (UM) and its generalized form (GUM) [5, 6] and the Hirota bilinear form method [7–31]. Among the methods, the Hirota's bilinear method is one of the most direct, basic and convenient tools to retrieve exact solitons, multi-soliton even collision of solitons solutions of NLEEs. While a NLEE can be reduced to its bilinear form, Lax pairs, lump solutions, multiple soliton and diverse interaction solutions of the equation can be achievable [11,15–35].

Nowadays, researchers are highly impressed to derive rogue/lump wave solutions for it's international interesting in the fields of plasma, deep ocean, nonlinear optics and Bose–Einstein condensates [16–18]. In 2002, Lou *et al* deliberated the lump solution by the use of the separation of variable scheme [19]. Very recently, Ma *et al* retrieved a general class of lump type solution of KPI model [20]. Other integrable models, which hold the lump solutions in the literature such as Boussinesq equation [21], BKP equation [22], the Davey–Stewartson equation II [23], the Ishimori-I equation [24] and so on. As a kind of articulate functioning outcomes, lump-type [11, 25, 26] solutions are localized in everydirection in the space. Rogue waves [27–32] are localized in both space and time, and come from nowhere and vanish without a trace [33], have taken the obligation of frequent marine disasters in the ocean engineering. Beside this, Liu *et al* [34–37] studied some nonlinear equations by using bell polynomials and with the aid of symbolic computation. Some rational type, soliton, lump and interaction solutions are presented. Dai et al [38–40], gave the interaction solutions between double breather wave solutions and the rogue wave solutions of $(2 + 1)$-dimensional coupled Nonlinear Schrödinger equation. Wang et al [41] studied wick-type stochastic fractional NLSE and gave various types soliton solutions. They also made various graphical analyses on the presented solutions to realize dynamics.

Inspired by the above works and mechanism of interaction solutions, we focus on the interaction solutions of the $(3 + 1)$-dimensional generalized B-typeKadomtsev-Petviashvili (gBKP) equation [42]

$$u_{yt} + 3u_{xz} - 3u_x u_{xy} - 3u_{xx}u_y - u_{xxxy} = 0. \tag{1}$$

Through the dependent variable transformation

$$u = 2(\ln \phi)_x = \frac{2\phi_x}{\phi}, \tag{2}$$

the $(3 + 1)$-dimensional gBKP equation can be convert to the bilinear D-operator form

$$(D_y D_t + 3D_x D_z - D_y D_x^3)(\phi \cdot \phi) = 0, \tag{3}$$

where $\phi = \phi(x, y, z, t)$ and the derivatives D_x, D_y, D_z, D_t are the Hirota's bilinear operators [7] defined in

$$D_x^\alpha D_y^\beta D_z^\gamma D_t^\delta(\phi \cdot \varphi) = \left(\frac{\partial}{\partial x} - \frac{\partial}{\partial x'}\right)^\alpha \left(\frac{\partial}{\partial y} - \frac{\partial}{\partial y'}\right)^\beta \left(\frac{\partial}{\partial z} - \frac{\partial}{\partial z'}\right)^\gamma \left(\frac{\partial}{\partial t} - \frac{\partial}{\partial t'}\right)^\delta.$$
$$\times\ \phi(x, y, z, t) \cdot \varphi(x', y', z', t')|_{x=x', y=y', z=z', t=t'}$$

Several researchers studied on the gBKP equation (1) in many ways such as: Ma and Zhu [43] explored multiple wave solutions of equation (1) via the multiple exp-function scheme. Liu et al [44] presented new exact non-traveling wave solutions by exploitation of the generalized (G'/G)-expansion method. Ma [45] constructed N-soliton solutions of equation (1) via the Hirota method. Recently, Cao [42] presented only lump wave solutions of the model.

The chief aimed of this paper is to present novel nonlinear dynamics as mixed lump-stripe collisions, novel breather behavior, single lump wave from the breather waves and various dynamical of collision with fission properties wave solutions for gBKP equation via suitable ansatzes approach.

2. Interaction phenomena between solitary and lump waves

In this section, we explore the dynamics of collisions between lump soliton and one stripe soliton of gBKP model (1). For this, we choose $\phi(x, y, z, t)$ as a combination of two positive quadratic functions and an exponential function as

$$\phi = g^2 + h^2 + a_{11} + \lambda\mu, \tag{4}$$

where

$$g(x, y, z, t) = a_1 x + a_2 y + a_3 z + a_4 t + a_5,$$

$$h(x, y, z, t) = a_6 x + a_7 y + a_8 z + a_9 t + a_{10},$$

and

$$\mu = \exp(k_1 x + k_2 y + k_3 z + k_4 t),$$

where $a_i (i = 1,\ldots,11)$, k and $k_i (i = 1,\ldots,4)$ are real factors to be later calculated. Plugging equation (4) into equation (3), and with a direct symbol calculation, we acquire 6 classes of solutions. We only select one of them to analyze characters of the similar solutions.

$$a_2 = a_3 = a_6 = a_9 = k_2 = k_3 = 0,\ a_4 = -\frac{3a_1 a_8}{a_7},\ k_4 = \frac{k_1(-3a_8 + a_7 k_1^2)}{a_7}, \tag{5}$$

with $a_7 \neq 0$.

Combining equation (5) and (4), we obtain the expression of $\phi(x, y, z, t)$:

$$\phi = \left(a_1 x - \frac{3ta_1 a_8}{a_7} + a_5\right)^2 + (a_7 y + a_8 z + a_{10})^2 + a_{11} + \lambda e^{k_1 x + \frac{k_1(-3a_8 + a_7 k_1^2)t}{a_7}}, \tag{6}$$

which, consecutively, produces the interaction of lump and stripe solitons to equation (1) through the transformation (2) as:

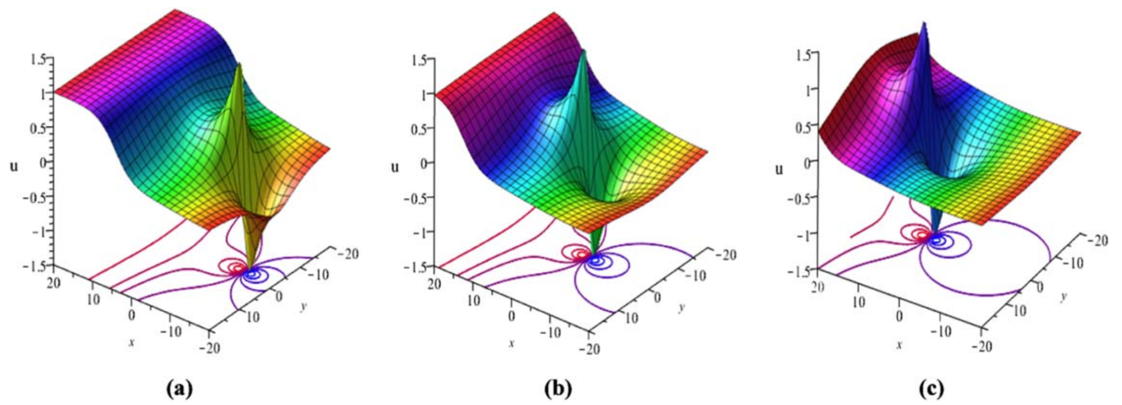

Figure 1. Profiles of solution (7) for equation (1) with $a_1 = a_7 = 1,\ a_5 = 3, a_8 = a_{10} = 2, a_{11} = 1.5,\ \lambda = 1.25$ (a) $t = -1.5$, (b) $t = 0$, and (c) $t = 1.5$ respectively for $z = 0$.

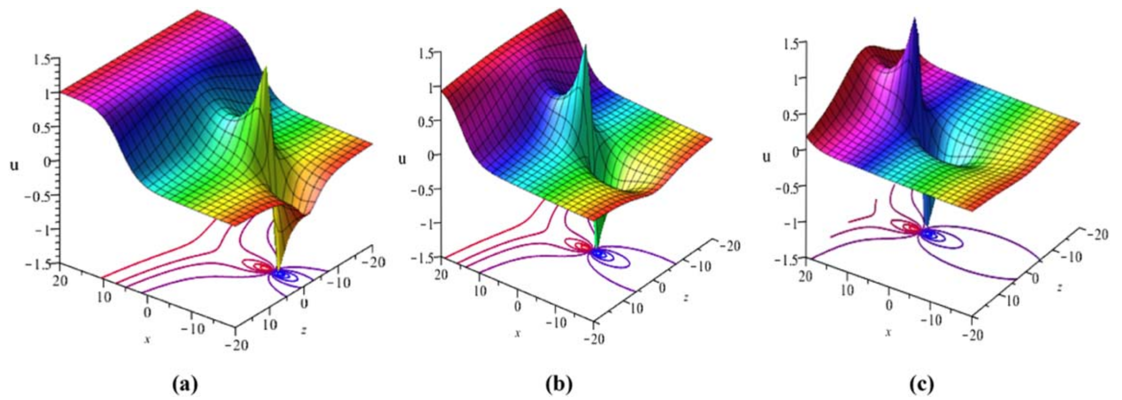

Figure 2. Profiles of solution (7) for equation (1) with $a_1 = a_7 = 1,\ a_5 = 3, a_8 = a_{10} = 2, a_{11} = 1.5,\ \lambda = 1.25$ (a) $t = -1.5$, (b) $t = 0$, and (c) $t = 1.5$ respectively for $y = 0$.

$$u_1 = \frac{2\left(2\left(a_1 x - \frac{3ta_1a_8}{a_7} + a_5\right)a_1 + \lambda k_1 e^{k_1 x + \frac{k_1(-3a_8+a_7k_1^2)t}{a_7}}\right)}{\left(a_1 x - \frac{3ta_1a_8}{a_7} + a_5\right)^2 + (a_7 y + a_8 z + a_{10})^2 + a_{11} + \lambda e^{k_1 x + \frac{k_1(-3a_8+a_7k_1^2)t}{a_7}}}. \tag{7}$$

In what follows, figure 1 present particular solution of equation (7) in $xy-$ plane and figure 2 presents this in the $xz-$ plane at dissimilar times by appropriate parameters selection. Curved lines strained in the bottom of the 3D figures are its corresponding contour plots.

3. Breather-wave solutions

In this section, we spotlight on the breather-wave solutions of equation (1) that comes from the collisions between exponential and trigonometric functions.

Case 1. Here, we take $\varphi(x, y, z, t)$ as a combination of a cosine function with two exponential functions:

$$\phi = e^{-\eta} + h_1 e^{\eta} + h_2 \cos(\xi), \tag{8}$$

with

$$\begin{aligned} \eta(x, y, z, t) &= p_1(r_1 x + a_1 y + b_1 z + c_1 t),\\ \xi(x, y, z, t) &= p_2(r_2 x + a_2 y + b_2 z + c_2 t), \end{aligned} \tag{9}$$

where $a_i, b_i, c_i, p_i, r_i, h_i, (i = 1, 2)$ are parameters to be designated later. Plugging equation (8) along with equation (9) into equation (3), with the help of symbolic computation system Maple, we achieve

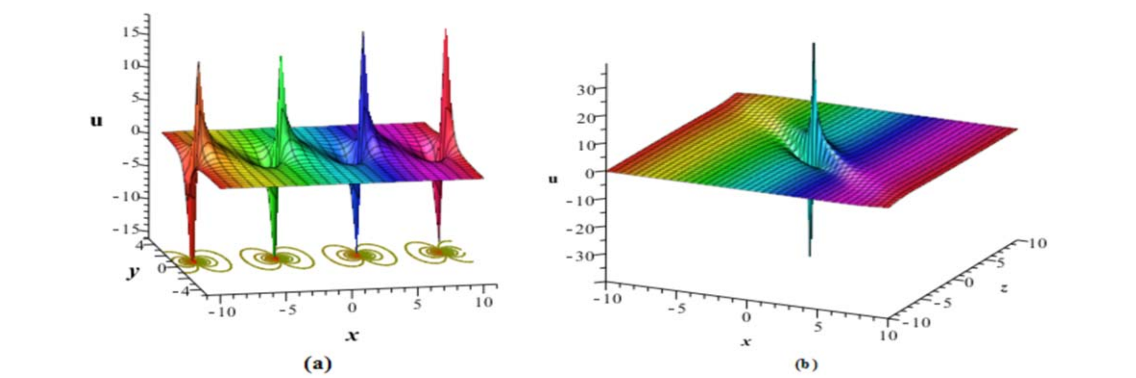

Figure 3. Profiles of solution (12) for equation (1) with $a_1 = b_2 = c_2 = p_1 = r_2 = p_1 = h_2 = 1$ **at** $t = 0$: (a) Perspective view of the wave for $z = 0$, and (b) degeneration of (12) by parametric limit of the wave equation (14) when and $y = 0$.

$$r_1 = a_2 = 0,\ b_1 = -\frac{1}{3}\frac{a_1(r_2^3 p_2^2 + c_2)}{r_2},\ c_1 = \frac{3b_2 r_2 p_2^2}{a_1 p_1^2},\ h_1 = \frac{1}{4}h_2^2, \tag{10}$$

which needs to satisfy the following conditions $a_1 \neq 0,\ p_1 \neq 0$ and $r_2 \neq 0$.

Setting equation (10) along with equation (9) into equation (8), we obtain the expression of $\phi(x, y, z, t)$, which is

$$\phi = e^{-p_1\Delta} + \frac{1}{4}h_2^2 e^{p_1\Delta} + h_2 \cos(p_2(c_2 t + r_2 x + b_2 z)). \tag{11}$$

Finally, inserting equation (11) into equation (2), we attain a periodic lump solution of the (3 + 1)-D gBKP equation

$$u_2 = \frac{-2h_2 p_2 r_2 \sin(p_2(c_2 t + r_2 x + b_2 z))}{\left(e^{-p_1\Delta} + \frac{1}{4}h_2^2 e^{p_1\Delta} + h_2 \cos(p_2(c_2 t + r_2 x + b_2 z))\right)}. \tag{12}$$

with $\Delta = \frac{3tb_2 r_2 p_2^2}{a_1 p_1^2} + a_1 y - \frac{1}{3}\frac{a_1 z(r_2^3 p_2^2 + c_2)}{r_2}$.

Putting $h_2 = 2,\ p_2 = p_1$ and taking limit as $p_1 \to 0$, the equation (11) reduce to a perturbation solution

$$\phi = \left(\frac{3b_2 r_2 t}{a_1} + a_1 y - \frac{a_1 c_1 z}{r_2}\right)^2 + (c_2 t + r_2 x + b_2 z)^2. \tag{13}$$

Through the transformation (2), it reduces to a single lump wave solution as follows:

$$u_{Lump} = \frac{4r_2(c_2 t + r_2 x + b_2 z)}{\left(\frac{3b_2 r_2 t}{a_1} + a_1 y - \frac{a_1 c_1 z}{r_2}\right)^2 + (c_2 t + r_2 x + b_2 z)^2}. \tag{14}$$

In what follows, figure 3(a) presents exact solution viathe equation (12) by selecting the appropriate values of constants. The result illustrates the solitonic interaction between lump and periodic waves produce a breather waves solution. Curved lines strained at the bottom of these figures are corresponding contours. While figure 3(b) produces the shape of single lump wave degenerated from the solution equation (12) via parametric limit approach.

Case 2. In this case, we consider $\phi(x, y, z, t)$ as a combination of a sine function with two exponential functions:

$$\phi = e^{-\eta} + h_1 e^{\eta} + h_2 \sin(\xi), \tag{15}$$

where η and ξ have been defined in the first case. Again, inserting equation (15) into equation (3), with the help of symbolic computation system Maple, gives the following solution.

$$a_1 = b_1 = r_2 = c_2 = 0,\ c_1 = -\frac{1}{3}\frac{r_1(a_2 r_1^2 p_1^2 - 3b_2)}{a_2}, \tag{16}$$

which needs to satisfy the following condition $a_2 \neq 0$.

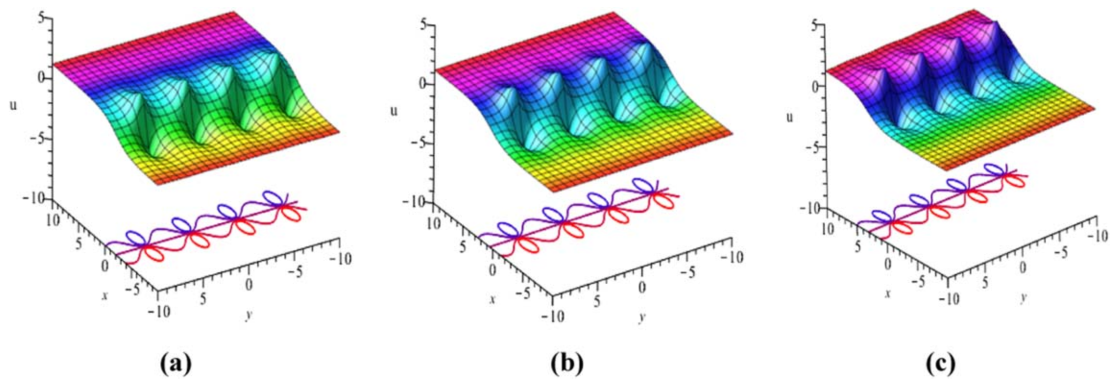

Figure 4. Profiles of solution (18) for equation (1) with $a_2 = b_2 = 1$, $r_1 = 2.5$, $h_1 = 0.5$, $h_2 = 1.2$, $p_1 = 0.25$, $p_2 = 1.25$: (a) $t = -1$, (b) $t = 0$, and (c) $t = 1$ respectively taking $z = 2$.

Setting equation (16) into equation (15), leads to the expression of $\phi(x, y, z, t)$:

$$\phi = e^{-p_1(\Delta_1 t + r_1 x)} + h_1 e^{p_1(\Delta_1 t + r_1 x)} + h_2 \sin(p_2(a_2 y + b_2 z)), \tag{17}$$

Finally, setting equation (15) into equation (2), we attain a periodic lump waves solution of the (3 + 1)-dimensional gBKP equation

$$u_3 = \frac{2(-p_1 r_1 e^{-p_1(\Delta_1 t + r_1 x)} + h_1 p_1 r_1 e^{p_1(\Delta_1 t + r_1 x)})}{e^{-p_1(\Delta_1 t + r_1 x)} + h_1 e^{p_1(\Delta_1 t + r_1 x)} + h_2 \sin(p_2(a_2 y + b_2 z))}, \tag{18}$$

with $\Delta_1 = \frac{r_1(a_2 r_1^2 p_1^2 - 3b_2)}{a_2}$.

The figure 4 interprets the wave shapes of the solution equation (18) with totally different parameters and consequently the curve exhausted below of the figure is the shape line. From the figures we see that the desired lump wave is $y -$ periodic and propagate along $x -$ direction as time goes.

4. Interaction solutions with fission phenomena

In this section, we spotlight on a new interaction solutions of equation (1). For this aim adopt a different test function [46] as follows:

$$\phi = G^2 + H^2 + a_9 + p\cosh(\xi_1) + q\cos(\xi_2), \tag{19}$$

where

$$G = a_1 x + a_2 y + a_3 z + a_4 t,\ H = a_6 x + a_7 y + a_8 z + a_9 t,$$
$$\xi_1 = m_1 x + m_2 y + m_3 t, \quad \xi_2 = k_1 x + k_2 y + k_3 t.$$

Here, $a_i (i = 1, 2, \ldots.., 9)$, $k_i (i = 1, 2, 3)$, p and q are real parameters while $m_i (i = 1, 2, 3)$ are real or imaginary constants. Plugging equation (19) into equation (3), via symbolic computation software Maple, we gain three sets of constraints. In the following, we analyze the three cases in details.

Case 1.

$$\begin{cases} a_1 = -\frac{a_6 a_5}{a_2},\ a_3 = -\frac{1}{3}\frac{a_2 a_8}{a_5},\ a_4 = -\frac{a_8 a_6}{a_2},\ a_7 = -\frac{1}{3}\frac{a_6 a_8}{a_5},\ k_3 = \frac{k_1(a_5 k_1^2 - a_8)}{a_5}, \\ m_3 = \frac{m_1(a_5 m_1^2 + a_8)}{a_5},\ k_2 = m_2 = 0, \end{cases} \tag{20}$$

where $a_2 \neq 0$ and $a_5 \neq 0$. Inserting equation (20) along with equation (19) into the equation (2), we advance into the interaction solution of equation (1):

$$u_4 = \frac{2\left(-\frac{2\chi_1 a_6 a_5}{a_2} + 2\chi_2 a_5 + p m_1 \sinh(t\chi_3 + m_1 x) + q k_1 \sin(t\chi_4 - k_1 x)\right)}{\chi_1^2 + \chi_2^2 + a_9 + p\cosh(t\chi_3 + m_1 x) + q\cos(t\chi_4 - k_1 x)}, \tag{21}$$

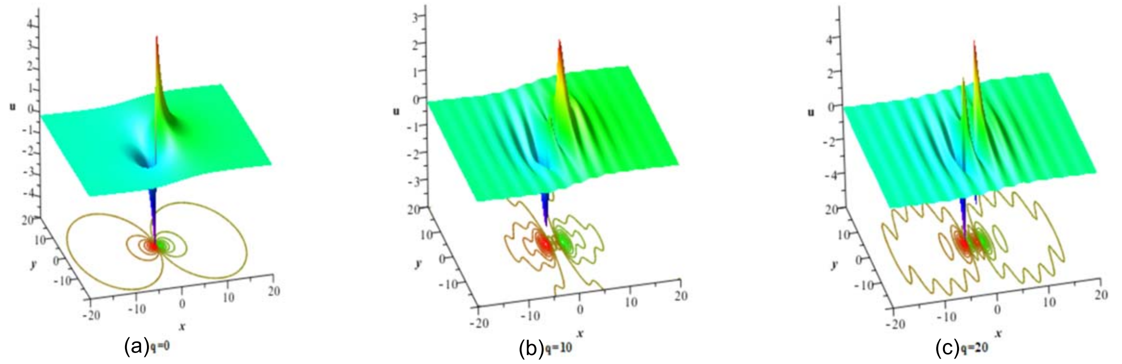

Figure 5. (Fission of lump wave) Profile of solution (21) for equation (1) with $a_2 = 1,\ a_5 = 2,\ a_6 = a_8 = 1.5,\ a_9 = 2,\ m_1 = 1,$ $k_1 = 2,\ p = 0,\ t = 0$ and $z = 0$.

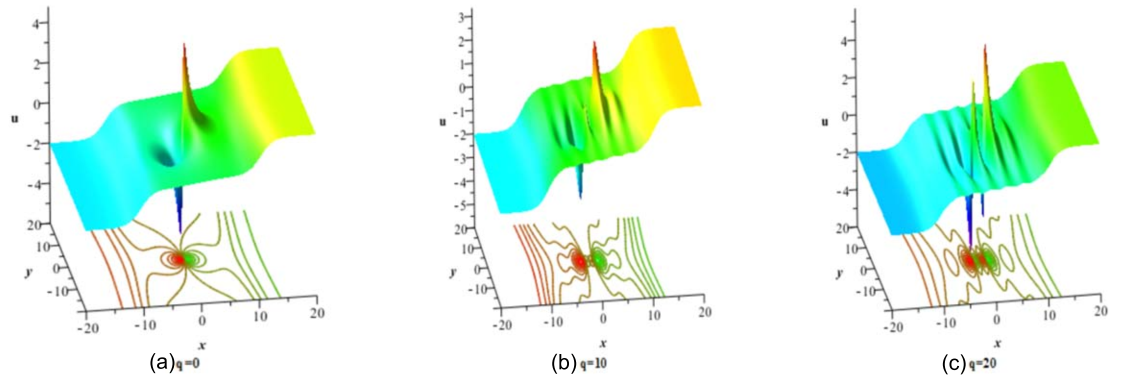

Figure 6. (Fission of lump wave) Profile of solution (21) for equation (1) with $a_2 = 1,\ a_5 = 2,\ a_6 = a_8 = 1.5,\ a_9 = 2,\ m_1 = 1,$ $k_1 = 2,\ p = \frac{1}{6}$ and $z = 0$: (a)$q = 0$; (b)$q = 10$, (c)$q = 20$.

where

$$\chi_1 = -\frac{ta_8a_6}{a_2} - \frac{xa_6a_5}{a_2} + a_2y - \frac{1}{3}\frac{za_2a_8}{a_5},\ \chi_2 = a_8t + a_5x + a_6y - \frac{1}{3}\frac{za_8a_6}{a_5},$$
$$\chi_3 = \frac{m_1(a_5m_1^2 + a_8)}{a_5} \text{ and } \chi_4 = \frac{k_1(a_5k_1^2 - a_8)}{a_5}.$$

Different conditions on the parameters p and q, u_4 (i,e., (21)) offers four different interaction solutions among the kinky, lumps and periodic waves. On the condition $p = 0$ and $q = 0$, u_4 exhibits a single lump solution (see figure 5(a)). It is known that a lump wave has one valley and one peak (see figure 5(a)). But for the parametric condition $p = 0$ and $q \neq 0$, u_4 (i,e., (21)) displays an interaction between a lump and a periodic wave (see figures 5(b)–(c)). In such case, the interaction between a lump and a periodic wave delivers one valley and one peak serially which split into two valleys and two peaks by fission (i.e. a fission phenomenon occurs for lump wave) as q gradually increases depicted in the figures 5(b)–(c). Fission of lump is cleared from the comparison of figures 5(b) and (c), as in figure 5(b) has one lump (one peak and one valley) and but in figure 5(c) has two lumps (two valleys and two peaks).

Due to the condition $p \neq 0$ and $q = 0$, u_4 (i,e., (21)) offers an interaction solitonic wave in which a lump get into a double kink waves (see figure 6(a)). Finally, on the condition $p \neq 0$ and $q \neq 0$, u_4 exposes an interaction among the lumps, double kinks and periodic waves. On observations of the figures 6(b)–(c), It is obvious that one valley and one peak of the lump (in figure 6(b)) split into two valleys and two peaks (in figure 6(c)) by fission as q increases into a double kinky periodic waves.

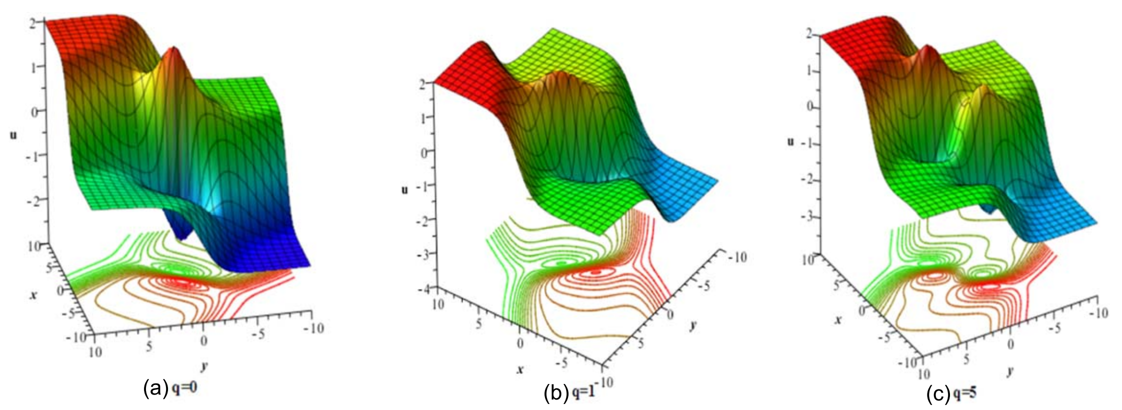

Figure 7. Profile of solution (23) for equation (1) with $a_2 = 1$, $a_5 = a_9 = 2$, $a_6 = a_8 = 1.5$, $m_1 = k_1 = k_3 = 1$, $p = 0.02$: (a) a lump get into a double kinky waves, (b) a lump going to fission that get into a double kinky waves and (c) a lump fission into two lump that get into a double kinky waves.

Case 2.

$$\begin{cases} a_3 = -\frac{1}{3}\frac{a_2(k_1^3 + k_3)}{k_1},\ a_7 = -\frac{1}{3}\frac{a_6(k_1^3 + k_3)}{k_1},\ m_3 = \frac{m_1(k_1^3 + m_1^2 k_1 + k_3)}{k_1}, \\ a_1 = a_4 = a_5 = a_8 = k_2 = m_2 = 0, \end{cases} \tag{22}$$

where $k_1 \neq 0$. Inserting equation (22) along with equation (19)into equation (2), we get the interaction solution of equation (1) as

$$u_5 = 2(\ln \phi)_x, \tag{23}$$

where,

$$\phi = \left(a_2 y - \frac{a_2(k_1^3 + k_3)}{3k_1} z\right)^2 + \left(a_6 x - \frac{a_6(k_1^3 + k_3)}{3k_1} y + a_9 t\right)^2 + a_9 + p\cosh(\xi_1) + q\cos(\xi_2),$$

$$\xi_1 = m_1 x + \frac{m_1(k_1^3 + m_1^2 k_1 + k_3)}{k_1} t,\ \xi_2 = k_1 x + k_3 t.$$

Case 3.

$$\begin{cases} a_4 = -\frac{3a_1 a_7}{a_6},\ k_3 = -\frac{k_1(3a_7 + a_6 k_1^2)}{a_6},\ m_3 = \frac{m_1(-3a_7 + a_6 m_1^2)}{a_6}, \\ a_2 = a_3 = a_5 = a_8 = k_2 = m_2 = 0, \end{cases} \tag{24}$$

where $a_6 \neq 0$. Inserting equation (24) along with equation (19) into equation (2), we get the interaction solution of equation (1).

$$u_6 = \frac{2\left(2\left(-\frac{3ta_1a_7}{a_6} + a_1 x\right)a_1 + pm_1\sinh(t\chi_5 + m_1 x) + qk_1\sin(t\chi_6 - k_1 x)\right)}{\left(-\frac{3ta_1a_7}{a_6} + a_1 x\right)^2 + (ya_6 + za_7)^2 + a_9 + p\cosh(t\chi_5 + m_1 x) + q\cos(t\chi_6 - k_1 x)}, \tag{25}$$

where

$$\chi_5 = \frac{m_1(-3a_7 + a_6 m_1^2)}{a_6},\ \chi_6 = -\frac{k_1(3a_7 + a_6 k_1^2)}{a_6}.$$

The solutions equations (23) and (25) have the similar four conditions like equation (21). The figure 7 presents specific solution equation (23) by selecting the appropriate values of constants that illustrate the interaction phenomena. If we agreed with $p \neq 0$ and $q = 0$ in equation (23), then we experience with an interaction between a lump and double kinky waves of equation (1) (see figure 7(a)). But If we agreed with $p \neq 0$ and $q \neq 0$ in equation (23), then weexperiencea fission phenomenon as $q \neq 0$ increases, in which lump waves split into more than one lump waves get into a double kinky wave (see figures 7(b)–(c)). On comparison between the figures 7(b) and (c), It is obvious that one valley and one peak of the lump (in figure 7(b)) split into two valleys and two peaks (in figure 7(c)) by fission as q increases that get into a double kinky periodic waves.

5. Results and discussions

We have successfully determined three types of interaction solutions among the lump, kink and periodic waves for the $(3 + 1)$-D gBKP model. But Ma and Zhu [43] explored multiple wave solutions of equation (1) via the multiple exp-function scheme. Liu *et al* [44] presented new exact non-traveling wave solutions by exploitation of the generalized (G'/G)-expansion method. Ma [45] constructed N-soliton solutions of equation (1) via the Hirota method. Recently, Cao [42] presented only lump wave solutions of the model. Meanwhile, we derive breather waves from interactions: hyperbolic functions with sinusoidal functions, collisions among exponential, hyperbolic and sinusoidal functions; single lump wave degenerated from the breather waves. Finally, we obtained interaction of lump wave, hyperbolic and sinusoidal functions with fission phenomena. We also illustrated the effect on lump wave increasing / decreasing the values of coefficients of hyperbolic or sinusoidal functions which has potential application to control the height of lump waves.

6. Conclusions

In this work, we investigate a generalized $(3 + 1)$-dimensional B-type Kadomtsev-Petviashvili model by the Hirota's bilinear method. With the aid of Maple-18, we have acquired some interactions solutions such as the lump-kink wave solution equation (7), breather-waves solutions equations (12) and (18) of the model. Also, we have presented some new interaction solutions among lump, kink and periodic wave solutions equations (21), (23) and (25) via a different 'rational-cosh-cos' type test functions. Moreover, we derive a single lump wave solution equation (14) by parametric limit approach that degenerate from the breather wave solution equation (12). Four different conditions on the exits parameters of the solutions equations (21), (23) and (25) are given to illustrate fission properties of lump waves into kink waves. To reveal the characteristics (fission, evolutions and flow patterns) of the obtained results, we present adequate 3D and contour graphical (figures 1–7) of the model. The gained solutions show that the enforced test functions procedure suggests a direct and easy scientific apparatus to manage any nonlinear problems arising in engineering problems and other applied fields. Some other interactions in [47] and multi-exponential wave solutions from weight functions in [48] are novel dynamical of fission-fusion phenomena that are our future task of the model.

Data availability statement

No new data were created or analysed in this study.

Compliance with ethical standards

The authors have no conflict of interest.

ORCID iDs

M Belal Hossen https://orcid.org/0000-0002-5748-7847
Harun-Or Roshid https://orcid.org/0000-0002-1687-623X

References

[1] Ablowitz M J and Clarkson P A 1991 *Solitons, Nonlinear Evolution Equations and Inverse Scattering* (New York: Cambridge University Press) (https://doi.org/10.1017/CBO9780511623998)
[2] Matveev V B and Salle M A 1991 *Darboux Transformations and Solitons* (Berlin: Springer) (https://doi.org/10.1007/978-3-662-00922-2)
[3] Yu G F and Tam H W 2008 *J. Math. Anal. Appl.* **344** 593–600
[4] Hossen M B, Roshid H O and Ali M Z 2017 *Int. J. Appl. Comput. Math.* **3** 1–19
[5] Gawad H I 2012 *J. Stat. Phys.* **147** 506
[6] Osman M S 2017 *Nonlinear Dyn.* **87** 1209–16
[7] Hirota R 2004 *The Direct Method in Soliton Theory* (Cambridge: Cambridge University Press) (https://doi.org/10.1017/CBO9780511543043)
[8] Roshid H O and Ma W X 2018 *Phys. Lett.* A **382** 3262–8
[9] Yan X W, Tian S F, Dong M J and Zhang T T 2018 *Comput. Math. Appl.* **76** 179–86
[10] Gilson C R and Nimmo J J C 1990 *Phys. Lett.* A **147** 472–6
[11] Peng W Q, Tian S F and Zhang T T 2018 *Phys. Lett.* A **382** 2701–8
[12] Liu Y and Wen X 2018 *Mod. Phys. Lett.* B **32** 1850161
[13] Cheng L and Zhang Y 2017 *Mod. Phys. Lett.* B **31** 1750224
[14] Liu J G, Zhu W H, Osman M S and Ma W X 2020 *Eur. Phys. J. Plus* **135** 412

[15] Khatun M S, Hoque M F and Rahman M A 2017 *Pramana—J. Phys.* **88** 86
[16] Hossen M B, Roshid H O and Ali M Z 2018 *Phys. Lett.* A **382** 1268–74
[17] Qin C Y, Wang X B, Tian S F and Zhang T T 2018 *Comput. Math. Appl.* **75** 4221–31
[18] Zhao Z L, Chen Y and Han B 2017 *Mod. Phys. Lett.* B **31** 1750157
[19] Lou S Y and Tang X Y 2006 *Nonlinear mathematical physics method* (Beijing: Academic)
[20] Ma W X 2015 *Phys. Lett.* A **379** 1975–8
[21] Ma H C and Deng A P 2016 *Commun. Theor. Phys.* **65** 546–52
[22] Yang J Y and Ma W X 2016 *Int. J. Mod. Phys.* B **30** 1640028 (1-7)
[23] Satsuma J and Ablowitz M J 1979 *J. Math. Phys.* **20** 1496–503
[24] Imai K 1997 *Progr. Theoret. Phys.* **98** 1013–23
[25] Wang H 2018 *Appl. Math. Lett.* **85** 27–34
[26] Ma W X 2016 *Int. J. Nonlinear Sci. Numer. Simul.* **17** 355–9
[27] Yue Y, Huang L and Chen Y 2018 *Comput. Math. Appl.* **75** 2538–48
[28] Li X, Wang Y, Chen M and Li B 2017 *Adv. Math. Phys.* **2017** 1743789
[29] Chen M D, Li X, Wang Y and Li B 2017 *Commun. Theor. Phys.* **67** 595
[30] Wen L L and Zhang H Q 2016 *Nonlinear Dyn.* **86** 877–89
[31] Roshid H O, Khan M H and Wazwaz A M 2020 *Heliyon* **6** e03701
[32] Hossen M B, Roshid H O and Ali M Z 2019 *Heliyon* **5** e02548
[33] Akhmediev N, Ankiewicz A and Taki M 2009 *Phys. Lett.* A **373** 675–8
[34] Liu J G and He Y 2018 *Nonlinear Dyn.* **92** 1103–8
[35] Liu J G, Eslami M, Rezazadeh H and Mirzazadeh M 2019 *Nonlinear Dyn.* **95** 1027–33
[36] Yin Y H, Ma W X, Liu J G and Lu X 2018 *Comput. Math. Appl.* **76** 1275–83
[37] Liu J G 2018 *Appl. Math. Lett.* **86** 36–41
[38] Dai C Q and Zhang J F 2020 *Nonlinear Dyn.* **100** 1621–8
[39] Dai C Q, Wang Y Y and Zhang J F 2020 *Nonlinear Dyn.* **102** 379–91
[40] Wu G Z and Dai C Q 2020 *Appl. Math. Lett.* **106** 106365
[41] Wang B H and Wang Y Y 2020 *Appl. Math. Lett.* **110** 106583
[42] Cao X F 2018 *Adv. Math. Phys.* **2018** 7843498
[43] Ma W X and Zhu Z N 2012 *Appl. Math. Comput.* **218** 11871–9
[44] Liu S, Ding Y and Liu J G 2017 *Int. J. Nonlinear Sci. Numer. Simul.* **18** 137–44
[45] Ma W X and Fan E G 2011 *Comput. Math. Appl.* **61** 950–9
[46] He C, Tang Y and Ma J 2018 *Comput. Math. Appl.* **76** 2141–7
[47] Chen S J, Lu X and Ma W X 2019 *Commun. Nonl. Sci. Numer. Simul.* **83** 105135
[48] Xu H N, Ruan W Y, Zhang Y and Lu X 2020 *Appl. Math. Lett.* **99** 105976